metals

MDPI

Article

Electrochemical Corrosion Resistance of Mg Alloy ZK60 in Different Planes with Respect to Extrusion Direction

G. Keerthiga [1,2,3], Dandapani Vijayshankar [2], MJNV Prasad [2], Mirco Peron [4], Jafar Albinmousa [5] and RK Singh Raman [3,*]

1 IITB-Monash Research Academy, Mumbai 400076, Maharashtra, India; keerthiga.ganesan@monash.edu
2 Department of Metallurgical Engineering and Materials Science, Indian Institute of Technology Bombay, Mumbai 400076, Maharashtra, India; v.dandapani@iitb.ac.in (D.V.); mjnvprasad@iitb.ac.in (M.P.)
3 Department of Chemical and Biological Engineering, Monash University, Clayton, VIC 3800, Australia
4 Department of Mechanical and Industrial Engineering, Norwegian University of Science and Technology, Høgskoleringen 1, 7034 Trondheim, Norway; mirco.peron@ntnu.no
5 Mechanical Engineering Department, King Fahd University of Petroleum & Minerals, Dhahran 31261, Saudi Arabia; binmousa@kfupm.edu.sa
* Correspondence: raman.singh@monash.edu

Abstract: The electrochemical corrosion resistance of a Mg-Zn-Zr alloy, ZK60, in different planes with respect to the extrusion direction was investigated in 3.5 wt% NaCl. The motivation of this study lies in the influence of extrusion on the grain size, texture and precipitation characteristics of magnesium alloys, and the profound role of these characteristics in the corrosion resistance of the alloys. Corrosion resistance was found to be considerably superior in the plane transverse to the extrusion direction (TD) than in the extrusion direction (ED) or normal to the extrusion direction (ND). The difference in the corrosion resistance was attributed to the variations in microstructural features in the TD, ED and ND directions.

Keywords: magnesium alloys; ZK60 alloy; extrusion; electrochemical corrosion

Citation: Keerthiga, G.; Vijayshankar, D.; Prasad, M.; Peron, M.; Albinmousa, J.; Singh Raman, R. Electrochemical Corrosion Resistance of Mg Alloy ZK60 in Different Planes with Respect to Extrusion Direction. *Metals* **2022**, *12*, 782. https://doi.org/10.3390/met12050782

Academic Editors: Frank Czerwinski and Sebastian Feliú, Jr.

Received: 12 March 2022
Accepted: 26 April 2022
Published: 30 April 2022

1. Introduction

Because of their high strength-to-weight ratios, magnesium (Mg) alloys are attractive for lightweight applications (such as aerospace and automobile). However, their poor resistance to electrochemical corrosion and creep deformation limits their wider use. It is intriguing that the high corrosion susceptibility (along with excellent biocompatibility) of Mg can be exploited for the use of Mg alloys for construction of biodegradable temporary implants, such as plates, pins, wires, screws, etc. The idea in such applications is to let the implant material dissolve away harmlessly within the human body after it has performed its temporary function, thereby entirely avoiding a surgical procedure for removal of the implant.

In the applications identified in the preceding description, Mg alloys are generally used in extruded form, in order to incorporate suitable microstructural/textural features that enhance the mechanical properties, such as strength and creep resistance. However, such microstructural variations in Mg alloys that are developed upon extrusion also profoundly influence alloys' corrosion resistance [1–3]. The microstructural/textural features that have the most profound influence on the corrosion of Mg alloys are the crystallographic variations in the different planes with respect to the extrusion direction, grain size and the aspects of the secondary precipitates that are developed for the purpose of strengthening. In almost all Mg alloys, the alloy matrix, i.e., the α-solid solutions, behaves anodic to the secondary phase (intermetallic) precipitates, and hence, the highly cathodic secondary precipitates cause severe localised corrosion to the adjoining anodic matrix [4–12]. In order to address the profound role of secondary precipitates in causing localised corrosion,

suitable surface engineering is required for the purpose of suppression of secondary precipitation to the surface microstructure of the alloy (while retaining the precipitates in the bulk microstructure for the strengthening) [13–32].

It is well-known that extrusion causes marked variations in the characteristics of secondary precipitates and grain size. However, studies on the role of the microstructural/textural variations in the different planes with respect to the extrusion direction on corrosion of Mg alloys are limited [1–3,33]. Jian et al. [1] reported variations in the corrosion rate of an aluminium- and zinc-containing Mg alloy, AZ80 alloy, in the extrusion direction (ED), the normal to extrusion direction (ND) and the transverse to extrusion direction (TD). They attributed this behaviour to the difference in the morphology of the secondary precipitates (viz., $Mg_{17}Al_{12}$) in the ED, ND and TD materials. The continuous network of the precipitate that developed in ED provided a physical barrier and superior corrosion resistance; the improvement in corrosion resistance due to such network is consistent with the observation of Song et al. [9]. However, the precipitates that developed in ND and TD material were discontinuous and caused severe corrosion to the adjoining alloy matrix [1]. Contrary to the findings of Jian et al. [1], Wang et al. [3] reported for the extruded version of another aluminium + zinc-containing Mg alloy, AZ31, that the corrosion rate was faster in the ED direction (which is called 'RD' in the article) than in the TD direction, whereas the rate was fastest for ND. Very little has been reported on the corrosion behaviour of an extruded version of Al-free Mg alloys in different orientations with respect to the extrusion direction (i.e., in the ED, ND and TD materials) [2]. Such investigations are important because alloying with Al is well known to enhance the corrosion of Mg alloys. Zheng et al. [2] reported a considerable difference in corrosion resistance between the regions of distinctly large and fine grain sizes that developed upon extrusion in a zinc- and zirconium-containing Mg alloy, ZK60.

Given the relative dearth in the understanding of the roles of the different orientations with respect to the extrusion direction as well as the profound role of alloying with zirconium in refining the grain size of Mg alloy, it is necessary to investigate the corrosion behaviour of zinc- and zirconium-containing Mg alloy in different orientations with respect to the extrusion direction (i.e., ED, ND and TD).

This study presents the preliminary investigation into electrochemical corrosion resistance in different planes (i.e., ED, ND and TD) with respect to the extrusion direction of a Mg alloy with zinc and zirconium as alloying elements, ZK60, in 3.5 wt% NaCl. For exploring the mechanistic understanding of the corrosion behaviour, the extruded alloy was subjected to a specific heat treatment (HT), followed by corrosion testing.

2. Experimental Details

2.1. Test Alloy

Extruded rectangular bars of alloy ZK60 were received from the Norwegian University of Science and Technology (Trondheim, Norway). The nominal composition (wt%) of the alloy is 5% Zn and 0.37% Zr. Samples (5 mm thick) were sectioned from the extruded bar.

2.2. Alloy Microstructure

Phases in the alloy were characterised using CuKα radiation with a Panalytical Xpert-pro XRD instrument (PANalytical, Almelo, The Netherlands). For characterisation of the anisotropy in the microstructure, the extruded alloy was subjected to grinding successively with 600, 800, 1200, 1500, 2000 and 5000 grit SiC paper (STARCKE, Melle, Germany), using water as the lubricant. The different surfaces of the extruded alloy (as seen in Figure 1) were ultrasonically cleaned in ethanol for 10 min, followed by polishing with a cloth that was charged with 1 µm diamond paste (HMI [P] Ltd., Mumbai, India), using kerosene aerosol (Solar Diamond, India) as the lubricant, then final ultrasonic cleaning in ethanol for 10 min. The duly polished surfaces were etched using picral (2 g picric acid (Loba Chemie, Mumbai, India), 5 mL acetic acid (Merck, Mumbai, India), 5 mL distilled water, 25 mL ethanol (Gogia & Co, Mumbai, India)) reagent. The planes of symmetry in the alloy are

defined as the extrusion direction (ED), transverse direction (transverse to extrusion plane) (TD), and normal direction (normal to extrusion plane) (ND).

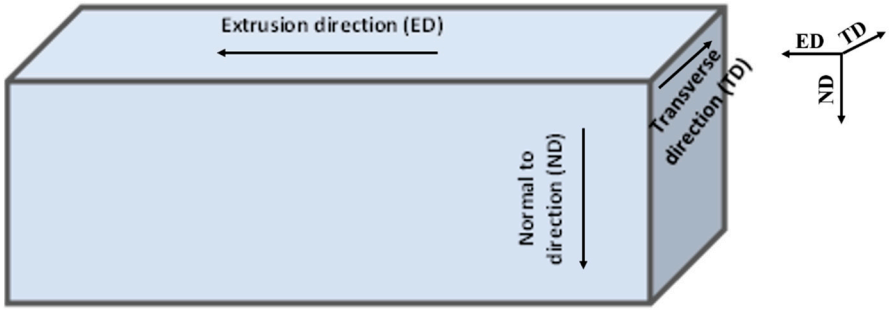

Figure 1. Schematic depiction of different orientations (ED, ND and TD) with respect to the extrusion direction of a ZK60 extruded bar.

The microstructural features were observed using an Olympus light microscope (Olympus life science). The line intercept method with a minimum of 300 measurements was carried out to calculate the average grain size and aspect ratio. Log normal distribution was employed to examine the statistical scatter in the grain size.

A few ED samples of $1 \times 1 \times 5$ cm^3 were subjected to annealing at 450 °C for 1 h (referred to as ED + HT), followed by furnace cooling. Continuous argon purging was employed for minimizing oxidation during the heat treatment.

2.3. Electrochemical Corrosion Measurement

Alloy samples of different orientations (ED, ND and TD) with respect to the extrusion direction were cold-mounted with only the specified orientation exposed (and other surfaces remaining masked within the mount). Potentiodynamic polarisation (PDP) of the cold-mounted samples was carried out in 3.5 wt% NaCl electrolyte, using a standard three-electrode setup using a Autolab potentiostat (PGSTAT302N, Metroohm, The Netherlands) and NOVA software (Version 2.8, Metroohm, The Netherlands). Silver/silver chloride (Ag/AgCl) and platinum coil (IPGI Instruments, Mumbai, India) were employed as reference and counter electrodes, respectively. Acrylic-mounted samples were polished using 600 grit SiC paper, rinsed with distilled water and air dried. The exposed sample area varied along different directions of ZK60, i.e., 1 cm^2 along the transverse plane (TD), 0.32 cm^2 along the short transverse plane (ND) and 0.4 cm^2 along the longitudinal plane (ED). The system was allowed to stabilize for 600 s before carrying out PDP in the range −0.3 V to +0.3 V with respect to open circuit potential (OCP) at a scan rate of 1 mV/s. The corrosion potential (Ecorr) and corrosion current density (Icorr) were determined upon Tafel extrapolation. PDP runs were at least duplicated for each condition, in order to examine reproducibility and determine the statistical deviations in the data.

3. Results and Discussion

3.1. Microstructure and Phase Composition of Extruded ZK60

Figure 2 shows the microstructure of the alloy in different planes (i.e., ED, ND and TD) with respect to the extrusion direction. As expected, the grains are elongated in the ED and ND planes. Grain size distribution in the different planes is also shown in Figure 2, whereas the average grain sizes are presented in Table 1.

XRD patterns obtained were matched with JCPDS (Joint Committee on Powder Diffraction Standards). Peaks in Figure 3 suggest the primary phase to be α-Mg, whereas the intermetallic phases identified were $MgZn_2$ and Zn_2Zr (which is consistent with those reported in the literature [1,2]).

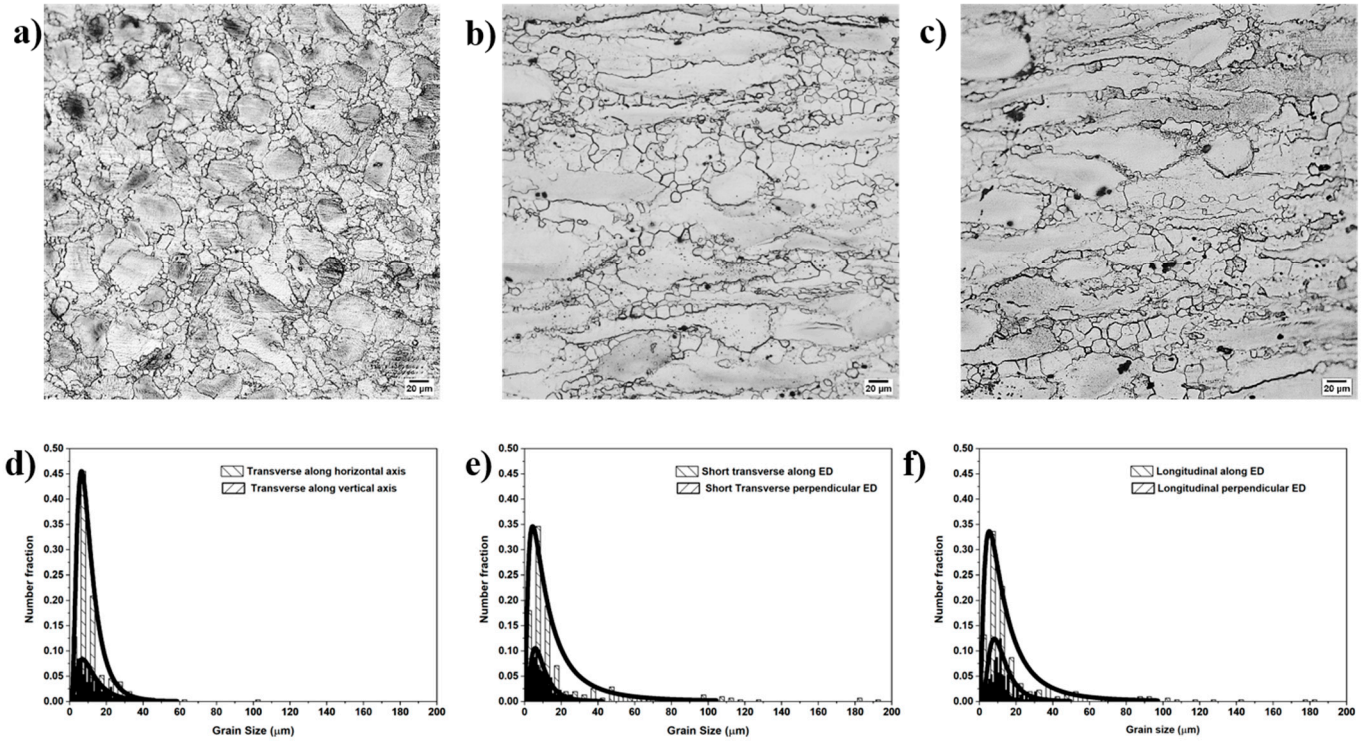

Figure 2. (**a**–**c**) Optical micrographs of the microstructure of ZK60 alloy in different planes (i.e., TD, ND and ED, respectively) with respect to the extrusion direction, and (**d**–**f**) the corresponding grain size distributions.

Table 1. Average grain size of ZK60 alloy in different planes with respect to the extrusion direction.

Orientation	Average Grain Size (μm)	Aspect Ratio
Extrusion direction (ED)	19 ± 1	1.5
Transverse to extrusion (TD)	13 ± 1	1
Normal to extrusion (ND)	20 ± 1	2

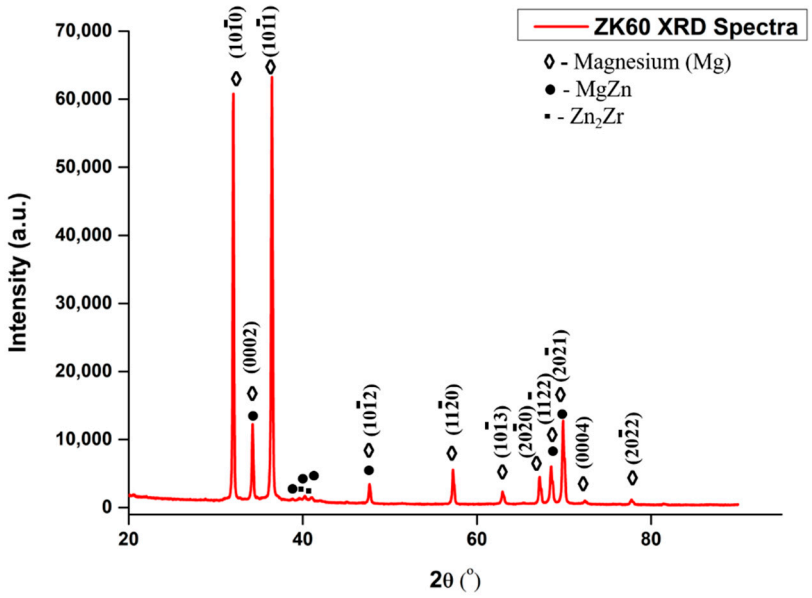

Figure 3. XRD spectrum of the extruded ZK60 alloy.

3.2. Corrosion Resistance of Extruded ZK60 in Different Planes

Figure 4 compares the potentiodynamic polarisation (PDP) behaviour of the extruded ZK60 alloy in different orientations with respect to the extrusion direction in 3.5 wt% NaCl. The I_{corr} and corrosion rate data that were extracted from the PDP curves in Figure 4 and presented in Table 2 suggest considerably greater corrosion resistance in the transverse (TD) plane than in the normal to extrusion (ND) and extrusion (ED) planes.

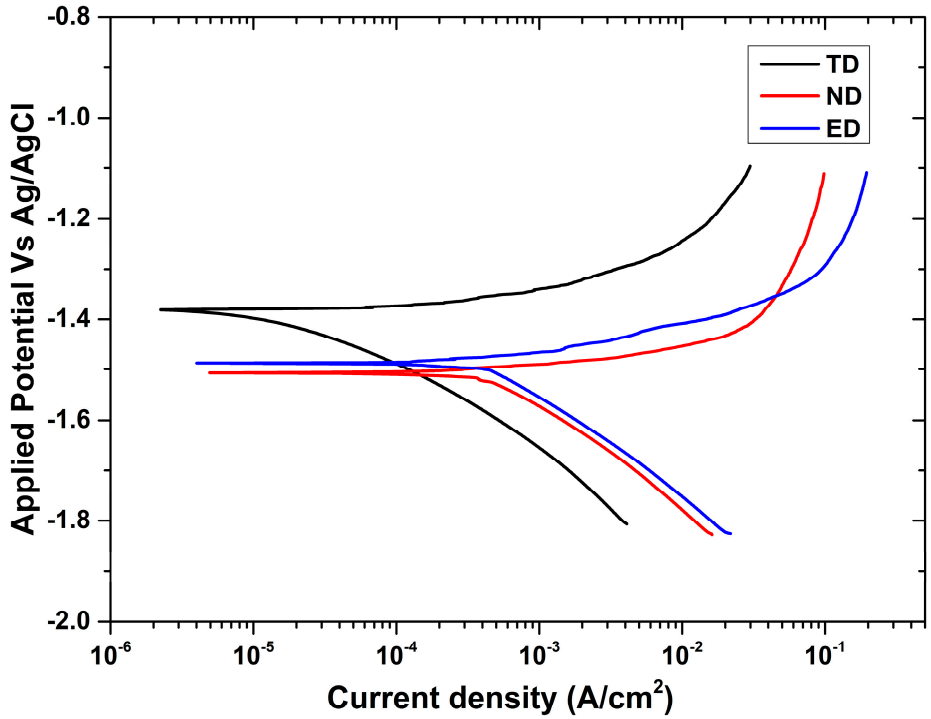

Figure 4. Potentiodynamic polarisation behaviour of the extruded ZK60 alloy in different planes with respect to the extrusion direction (i.e., ED, ND and TD) in 3.5 wt% NaCl.

Table 2. Icorr and corrosion rate data (extracted from the PDP curves in Figure 3) in TD, ND and ED planes of the extruded alloy ZK60.

Orientation	I_{corr} ($\mu A/cm^2$)	Corrosion Rate (mmpy)
Transverse to extrusion (TD)	73.69 ± 13.99	65
Normal to extrusion (ND)	526.33 ± 41.18	466
Extrusion direction (ED)	361.14 ± 87.96	320
ED + 450 °C/1 h (ED + HT)	0.02 ± 0.0005	1.8×10^{-2}

As discussed in the Introduction section, the corrosion resistance of Mg alloys is profoundly influenced by the grain size and the morphology of the secondary precipitates. Grain refinement often improves corrosion resistance. In this respect, the lower Icorr and corrosion rate in the TD (than in ND and ED planes) is consistent with the finer grain size in the TD plane (as seen in Figure 2 and Table 1). However, it is crucial to note that the morphology of the secondary precipitates has also been reported to vary considerably in different planes of Mg alloys. The common view is that the secondary precipitates, which are generally cathodic to the alloy matrix, deteriorate the corrosion resistance of Mg alloys [4–12]. However, Song et al. [9] and Jian et al. [1] demonstrated that when the secondary precipitates form a continuous network, they provide a physical barrier and improve the corrosion resistance of Mg alloys. In order to explore whether this mechanism could also contribute to the observed superior corrosion resistance in the TD plane (as seen in Figure 4 and Table 2), a few samples of the ED plane were subjected to annealing at

450 °C for 1 h, followed by furnace cooling, with a view to facilitating the development of a continuous network of precipitates. This treatment (i.e., 450 °C/1 h) is nominated as ED + HT. As seen in Figure 5 and Table 2, the corrosion resistance of the ED + HT samples is considerably superior than that of the alloy without this treatment (ED, ND or TD). Among the ED, ND or TD planes, the continuous nature of the secondary precipitates is likely in the TD plane (which shows superior corrosion resistance) than in the ED and ND planes where the directional stresses during extrusion may cause fragmentation of the precipitates. In order to validate the mechanism based on the continuous nature of the precipitates for the ED + HT and TD samples, some preliminary scanning electron microscopy (SEM) (GeminiSEM, Zeiss, Oxford) was carried out on the microstructure of ED and ED + HT samples. As seen in Figure 6, the morphology of the grain boundary precipitates in ED + HT seems to have greater continuity than in ED. However, it will be necessary to carry out comprehensive microscopy, which is a matter of further investigation.

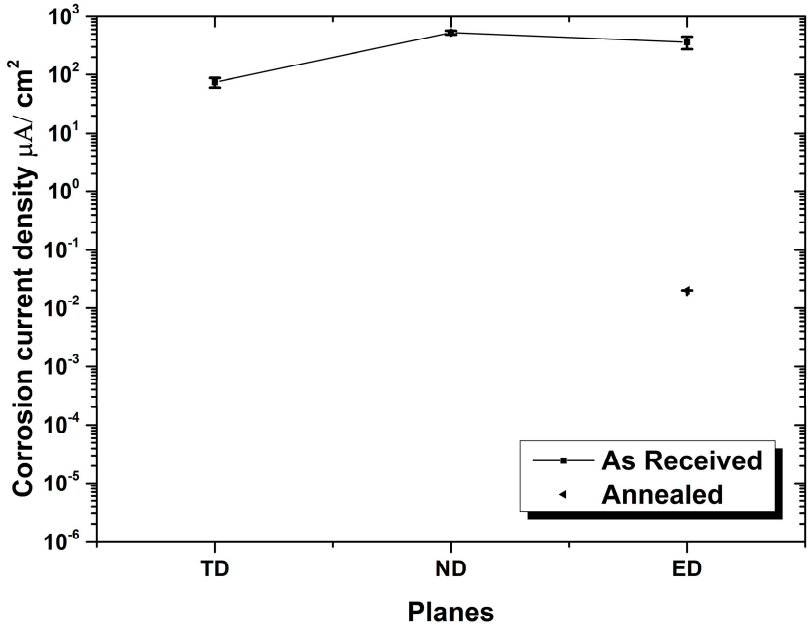

Figure 5. Comparison of corrosion current density of the heat-treated (450 °C/1 h) ED (i.e., ED + HT) with TD, ND and ED alloy in 3.5 wt% NaCl. Error bars are the standard deviation of the replicated measurements.

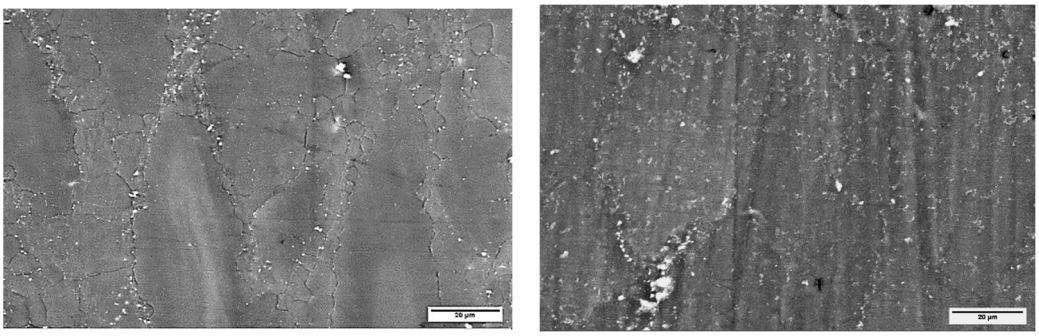

(**a**) (**b**)

Figure 6. SEM images of the microstructure of (**a**) ED and (**b**) ED + HT.

4. Conclusions

The electrochemical corrosion resistance of ZK60 alloy (a Mg-Zn-Zr alloy) was investigated in 3.5 wt% NaCl, in different planes with respect to the extrusion direction,

i.e., extrusion direction (ED), transverse to the extrusion direction (TD) and normal to the extrusion direction (ND). The main inferences of this study are as follows:

1. The TD plane was found to show considerably superior corrosion resistance than the ED and ND planes. The trend in corrosion resistance was TD > ED > ND.
2. The superior corrosion resistance of the TD plane is attributed to the greater likelihood of unfragmented secondary precipitates in this plane (than in ED and ND planes).
3. A specific heat treatment of ED samples that was designed to facilitate the development of a continuous network of secondary precipitates (which is reported in the literature to enhance the corrosion resistance of Mg alloys) was indeed found to considerably improve the corrosion resistance of the ED alloy.
4. Observation of the microstructure by scanning electron microscopy of ED and heat-treated ED samples provides preliminary confirmation of the mechanistic explanation.

Author Contributions: G.K., conceptualization and planning of the work, experimental work, data analyses and writing the manuscript; D.V., supervision, conceptualization and planning of the work, data analyses and technical discussions; M.P. (MJNV Prasad), supervision, conceptualization and planning of the work, data analyses and technical discussions; M.P. (Mirco Peron), supply of test material and technical discussions; J.A., supply of test material and technical discussions; and R.S.R., supervision, conceptualization and planning of the work, and writing the manuscript. All authors have read and agreed to the published version of the manuscript.

Funding: G.K. received a scholarship from Department of Biotechnology, India through IITB-Monash Research Academy to pursue this work.

Institutional Review Board Statement: Not applicable.

Informed Consent Statement: Not applicable.

Data Availability Statement: Data are contained within the article.

Conflicts of Interest: The authors declare no conflict of interest.

References

1. Jiang, Q.; Ma, X.; Zhang, K.; Li, Y.; Li, X.; Li, Y.; Ma, M.; Hou, B. Anisotropy of the crystallographic orientation and corrosion performance of high-strength AZ80 Mg alloy. *J. Magnes. Alloy.* **2015**, *3*, 309–314. [CrossRef]
2. Zenga, R.; Kainer, K.U.; Blawert, C.; Dietzel, W. Corrosion of an extruded magnesium alloy ZK60 component—The role of microstructural features. *J. Alloy. Compd.* **2011**, *509*, 4462–4469. [CrossRef]
3. Wang, B.J.; Xu, D.K.; Xin, Y.C.; Sheng, L.Y.; Han, E.H. High corrosion resistance and weak corrosion anisotropy of an as-rolled Mg-3Al-1Zn (in wt.%) alloy with strong crystallographic texture. *Sci. Rep.* **2017**, *7*, 16014. [CrossRef] [PubMed]
4. Raman, R.K.S. The role of microstructure in localized corrosion of magnesium alloys. *Metall. Mater. Trans. A* **2004**, *35*, 2525. [CrossRef]
5. Pebere, N.; Riera, C.; Dabosi, F. Investigation of magnesium corrosion in aerated sodium sulfate solution by electrochemical impedance spectroscopy. *Electrochim. Acta* **1990**, *35*, 555. [CrossRef]
6. Pardo, A.; Merino, M.C.; Coy, A.E.; Arrabal, R.; Viejo, F.; Matykina, E. Corrosion behaviour of magnesium/aluminium alloys in 3.5 wt.% NaCl. *Corros. Sci.* **2008**, *50*, 823. [CrossRef]
7. Das, S.K.; Davis, L.A. High performance aerospace alloys via rapid solidification processing. *Mater. Sci. Eng.* **1988**, *98*, 1. [CrossRef]
8. Song, G.; Atrens, A.; Xianliang, W.; Zhang, B. Corrosion behaviour of AZ21, AZ501 and AZ91 in sodium chloride. *Corros. Sci.* **1998**, *40*, 1769. [CrossRef]
9. Song, G.; Atrens, A.; Dargusch, M. Influence of microstructure on the corrosion of diecast AZ91D. *Corros. Sci.* **1998**, *41*, 249. [CrossRef]
10. Zhao, M.C.; Liu, M.; Song, G.L.; Atrens, A. Influence of Microstructure on Corrosion of As-cast ZE41. *Adv. Eng. Mater.* **2008**, *10*, 104. [CrossRef]
11. Neil, W.C.; Forsyth, M.; Howlett, P.C.; Hutchinson, C.R.; Hinton, B.R.W. Corrosion of magnesium alloy ZE41—The role of microstructural features. *Corros. Sci.* **2009**, *51*, 387. [CrossRef]
12. Neil, W.C.; Forsyth, M.; Howlett, P.C.; Hutchinson, C.R.; Hinton, B.R.W. Corrosion of heat treated magnesium alloy ZE41. *Corros. Sci.* **2011**, *53*, 3299. [CrossRef]
13. Izumi, S.; Yamasaki, M.; Kawamura, Y. Relation between corrosion behavior and microstructure of Mg-Zn-Y alloys prepared by rapid solidification at various cooling rates. *Corros. Sci.* **2009**, *51*, 395. [CrossRef]
14. Makar, G.L.; Kruger, J. Corrosion Studies of Rapidly Solidified Magnesium Alloys. *J. Electrochem. Soc.* **1990**, *137*, 414. [CrossRef]

15. Qian, M.; Li, D.; Jin, C. Microstructure and corrosion characteristics of laser-alloyed magnesium alloy AZ91D with Al-Si powder. *Sci. Technol. Adv. Mat.* **2008**, *9*, 025002. [CrossRef]
16. Volovitch, P.; Masse, J.E.; Fabre, A.; Barrallier, L.; Saikaly, W. Microstructure and corrosion resistance of magnesium alloy ZE41 with laser surface cladding by Al-Si powder. *Surf. Coat. Technol.* **2008**, *202*, 4901. [CrossRef]
17. Gao, Y.; Wang, C.; Lin, Q.; Liu, H.; Yao, M. Broad-beam laser cladding of Al-Si alloy coating on AZ91HP magnesium alloy. *Surf. Coat. Technol.* **2006**, *201*, 2701. [CrossRef]
18. Subramanian, R.; Sircar, S.; Mazumdar, J. Laser cladding of zirconium on magnesium for improved corrosion properties. *J. Mater. Sci.* **1991**, *26*, 951. [CrossRef]
19. Wang, A.A.; Sircar, S.; Mazumder, J. Laser cladding of Mg-AI alloys. *J. Mater. Sci.* **1993**, *28*, 5113. [CrossRef]
20. Majumdar, J.D.; Galun, R.; Mordike, B.L.; Manna, I. Effect of laser surface melting on corrosion and wear resistance of a commercial magnesium alloy. *Mater. Sci. Eng. A* **2003**, *361*, 119. [CrossRef]
21. Coy, A.E.; Viejo, F.; Garcia-Garcia, F.J.; Liu, Z.; Skeldon, P.; Thompson, G.E. Effect of excimer laser surface melting on the microstructure and corrosion performance of the die cast AZ91D magnesium alloy. *Corros. Sci.* **2010**, *52*, 387. [CrossRef]
22. Guan, Y.C.; Zhou, W.; Zheng, H.Y. Effect of laser surface melting on corrosion behaviour of AZ91D Mg alloy in simulated-modified body fluid. *J. Appl. Electrochem.* **2009**, *39*, 1457. [CrossRef]
23. Gao, Y.; Wang, C.; Yao, M.; Liu, H. Corrosion behavior of laser melted AZ91HP magnesium alloy. *Mater. Corros.* **2007**, *58*, 463. [CrossRef]
24. Guo, L.F.; Yue, T.M.; Man, H.C. Excimer laser surface treatment of magnesium alloy WE43 for corrosion resistance improvement. *J. Mater. Sci.* **2005**, *40*, 3531. [CrossRef]
25. Liu, S.Y.; Hu, J.D.; Yang, Y.; Guo, Z.X.; Wang, H.Y. Microstructure analysis of magnesium alloy melted by laser irradiation. *Appl. Surf. Sci.* **2005**, *252*, 1723. [CrossRef]
26. Abbas, G.; Liu, Z.; Skeldon, P. Corrosion behaviour of laser-melted magnesium alloys. *Appl. Surf. Sci.* **2005**, *247*, 347. [CrossRef]
27. Raman, R.K.S.; Murray, S.; Brandt, M. Laser assisted modification of surface microstructure for localised corrosion resistance of magnesium alloys. *Surf. Eng.* **2007**, *23*, 107. [CrossRef]
28. Koutsomichalis, A.; Saettas, L.; Badekas, H. Laser treatment of magnesium. *J. Mater. Sci.* **1994**, *29*, 6543. [CrossRef]
29. Dubé, D.; Fiset, M.; Couture, A.; Nakatsugawa, I. Characterization and performance of laser melted AZ91D and AM60B. *Mater. Sci. Eng. A* **2001**, *299*, 38. [CrossRef]
30. Majumdar, J.D.; Maiwald, T.; Galun, R.; Mordike, B.L.; Manna, I. Laser Surface Alloying of an Mg Alloy with Al + Mn to Improve Corrosion Resistance. *Laser. Eng.* **2002**, *12*, 147. [CrossRef]
31. Banerjee, P.C.; Raman, R.K.S.; Durandet, Y.; McAdam, G. Electrochemical investigation of the influence of laser surface melting on the microstructure and corrosion behaviour of ZE41 magnesium alloy—An EIS based study. *Corros. Sci.* **2011**, *53*, 1505. [CrossRef]
32. Durandet, Y.; Sun, S.; Brandt, M. Microstructure of Laser Treated ZE41A-T5 Magnesium Alloy. *Mater. Sci. Forum.* **2010**, *654*, 759–762. [CrossRef]
33. Bertolini, R.; Bruschi, S.; Ghiotto, A.; Pezzato, L.; Dabala, M. Large Scale Extrusion Machining of Magnesium Alloys for Bioimplant Applications. *Proceedia CIRP* **2018**, *71*, 105–110. [CrossRef]